Springer

Journal of Mechanical Science and Technology 22 (2008) 1620~1632

Journal of
Mechanical
Science and
Technology

www.springerlink.com/content/1738-494x
DOI 10.1007/s12206-008-0432-7

Phase doppler measurements: system set-up optimization for characterization of a diesel nozzle

Raul Payri[1,*], Lucio Araneo[2], Joseph Shakal[3] and Vlad Soare[1]

[1]*CMT Motores Termicos, Universidad Politecnica de Valencia, Valencia, E-46022, Spain*
[2]*Politecnico di Milano, Dipartimento di Energetica, via La Masa 34, 20156 Milano, Italy*
[3]*TSI Inc., 500 Cardigan Road, Shoreview, MN, 55126, USA*

(Manuscript Received November 7, 2007; Revised April 22, 2008; Accepted April 30, 2008)

Abstract

A commercial phase Doppler system was set up, optimized and used to measure the time resolved characteristics of the droplets inside a diesel spray. The purpose of this work was to understand exactly the influence of each system parameter, and to find the best setup enabling measurements in the spray zones that are densest and closest to the injector. Parametric studies were performed to gain an understanding of the particle density limits of the system and their dependence on the system parameters. Then the diesel spray produced by a single-hole injector was measured, with the fuel pressure ranging from 300 to 1300 bar and gas density in the test chamber ranging from ambient conditions to 40 kg/m^3. The optic parameters (beam waist size, lenses focal length) were chosen to the best expected values allowed by the optical stand-off of the spray enclosure. The receiver slit width, which was found to have a dramatic effect on the detection of droplets during the injection main period, was tested in the range from 100 μm to 25 μm. Tests were carried out with two different slit lengths, namely 1 mm and 50 μm, with results indicating minimal effect on performance. PMT voltage (gain) was held to a moderately low value between 400 and 500 V and the laser power between 400 and 800 mW in the green line. An optimum burst threshold was found to obtain the best quality data regardless of signal background level, which varies greatly in high-density pulsed sprays. In the end, a set of results from the complete nozzle characterization in various conditions is presented in order to show the practical application of the optimization study and to provide some means of appreciating the results accuracy. The results obtained were also used to show that the gas-jet theory can be used to predict if PDPA measurement are possible in a given experimental situation.

Keywords: Diesel, Droplet velocity; Droplet size; Phase doppler interferometry

1. Introduction

Understanding the process of fuel injection and combustion in diesel engines is crucial to attaining low pollutant emission levels together with high engine power and comfort performances, as it is required from a modern engine by national/local regulations and market demands [1]. For these purposes, a deeper knowledge of the spray characteristics is required of the fuel interaction with air and combustion and for more accurate CFD simulation of the fluid and thermodynamic processes. Laser Doppler velocimetry is a well-known and powerful technique able to measure the velocity and, under certain hypotheses, also the size of spherical particles like fuel droplets in the air [2]. The application of Phase Doppler anemometry in a diesel spray is quite challenging because of the specific characteristics of a diesel spray [3, 4]. The pulsed injections, with typical durations of milliseconds require time-resolved measurements with microsecond accuracy. The maximum speed of droplets is of the order of hundreds of meters per second, with very slow droplets in the spray pe-

*Corresponding author. Tel.: +34 963879658, Fax.: +34 963877659
E-mail address: rpayri@mot.upv.es

riphery and in the injector closing phases. This requires a very large dynamic range of measured velocity. The droplet size is also a challenging measurement. Since injection pressures are now typically from 1000 to 2000 bar, it can be expected a significant number of drops whose diameter is approaching the minimum instrument size limit (~0.5 μm). Since laser and phase Doppler measurements are strictly single-particle techniques, the high droplet concentration in the spray core requires a very small measurement volume to avoid burst splitting and other multiple particle events. Optical access is often made difficult by the surrounding droplets that attenuate and deflect the incoming laser beams as well as the scattered light signal, and thus signals originating from the smaller droplets could be very noisy or not even detected. Consequently, there is a risk of biasing the results toward larger droplet diameters. The necessity to measure the spray characteristics in an environment close to real injection conditions, namely gas high density and/or high temperature, requires use of a high-pressure test rig equipped with optical access. These optical windows are subject to fouling and are another source of light distortion, eventually resulting in noisier signals.

Even in the presence of all these constraints, it will be shown that an accurate study and optimization of the experimental set-up and of the operating parameters can lead to significant improvements of the results compared with what was previously achieved with this equipment [5].

In section 4 of the paper, a complete nozzle characterization is presented, showing consistency both within themselves and with theories and experimental results available throughout the literature. Finally, a new criterion to predict if measurements are possible in a given experimental situation could be deduced by comparing the experimental results to the gas-jet spray analogy.

2. Experimental setup

2.1 Injection system and test chamber

The injection test rig used is composed of a closed circuit with scavenging gas, where the fuel spray is injected, and optical access is provided through three perpendicular windows. The circuit can be kept open to atmospheric air, or closed and pressurized with air up to a density of 7 kg/m^3, or pressurized by sulphur hexafluoride (SF_6) up to 40 kg/m^3 obtained at 6 bar absolute pressure while keeping the pressure within the system limit.

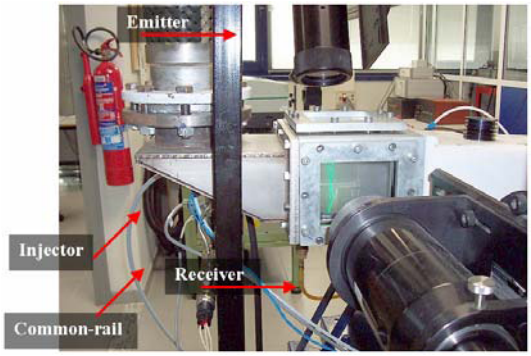

Fig. 1. The setup, with the transmitting optic from the top, the receiving optic horizontal, the injector from the left in the scavenging flow.

The spray is produced by a single-hole injector and is directed stream-wise in the gas flow; in this way window fouling is avoided and experiments can be run for many hours without the risk of signal degradation. An extended description of the set-up is given in [6]; the injector used in these tests has a nozzle outlet diameter of 110 μm; fuel was provided at constant pressure from 300 to 1300 bar, and the pulse duration to control the injector was selected between 1 and 4.5 ms; the injection repetition rate was 7 Hz. A picture of the experimental setup is shown in Fig. 1.

For preliminary setup tests a 4 mm diameter gas jet was used, while keeping the test rig at atmospheric conditions. The jet was generated by a TSI six-jet atomizer, using oil for seed particle generation, allowing LDV measurements up to 100 m/s.

2.2 Description of the PDPA system

The instrument used in this experiment is a TSI PDPA system, with an FSA4000 digital processor. Its main parameters are:

- Maximum measurable frequency: 175 MHz (corresponding to 243.6 m/s with current optical set-up) and without down-mixing of the incoming signal
- Minimum measurable frequency: 300 Hz (corresponding to -72.2 m/s with current optical set-up), without down-mixing
- Minimum transit time: 50 ns (this imposes an upper velocity limit of 1300 m/s)
- Maximum sampling rate: 800 MHz.

For a fully detailed explanation of phase Doppler

interferometry principles, one may refer to [7]. The expected velocities to be measured in the spray [8] were up to 100 m/s, depending on the injection and chamber pressures, with droplet size up to a few tens of micrometers, and high droplet concentration. The most important optical requirements are, then, a very small measurement volume with short fringe distance [9, 10]. In this work the PDPA was consequently used with the following configuration:

- Laser: Coherent Inc. – INNOVA 70 c series, argon-ion, single line mode (514.5 nm), for one-component velocity and diameter measurement.
- Bragg cell frequency (frequency shift): 40 MHz
- Transmitting optic focal length: 200 mm
- Beam separation at the front lens: 57.6 mm
- Beam diameter ($1/e^2$) at the front lens, after beam expander: 2 mm
- Fringe spacing: 1.8 μm
- Focused beam waist, nominal measurement volume diameter ($1/e^2$): 65 μm
- Receiving optic focal length: external 300 mm, internal for refocusing 250 mm
- Receiver's lenses effective diameter: 70 mm
- Scattering angle: 70º
- Slit aperture: 100, 50, and 25 μm (refocused on the measurement volume to +20%.)
- Velocity range: -36 to 244 m/s (with maximum filter bandwidth 20-175 MHz, without down-mixing)
- Diameter range: up to 70 μm, with fuel refractive index 1.44

After a preliminary choice of the optical configuration, the effort was focused upon the remaining optical parameters and most of the software parameters to be chosen with the goal of optimizing the results, by taking into account mainly the acquisition data-rate and the measured velocity and droplet diameter. Although the investigation was performed with a specific system, the parameters studied, both of hardware and software type, as well as the working principles are generally valid for any PDA system with only some details varying inherently from one manufacturer to another.

2.3 Available parameters and their main effect on the results

2.3.1 Laser power

When the laser power is too low, small particles are not detected, but when it is too high the largest particles can saturate the photomultiplier. The effective illuminated measurement volume becomes larger, increasing the background noise and the possibility that multiple scatter occurs. Values used ranged between 100 and 1000 mW at the laser source; each laser beam receives approximately 18% of this power in optimal conditions, the rest being lost in the transmission chain.

2.3.2 Window material

A window is always a source of laser attenuation and distortion, and scratches on its surface or droplets deposed on it act like scattering sources affecting the coherence of the laser beam. There were tested both plastic (methacrylate, 100 × 100 mm) and glass (borosilicate, Ilmadur, Φ80 mm).

2.3.3 Slit width and height

The slit aperture cuts the view of the ellipsoidal volume formed by the two intersecting laser beams, so that a smaller slit width helps decrease the measurement volume, which is useful when measuring inside a very dense spray. An excessively small slit of 5μm for example, much smaller than the droplet to be measured, could lead to strong diffraction and slit effects [7]. An easy way to further decrease the measurement volume size is to use a pin hole, or two overlapped slits crossing at 90º, but this solution makes it impossible to determine the effective measurement volume dimension. Slits of 100, 50 and 25 μm were tested, as was the 90º crossing of the 25 and 50 μm slits.

2.3.4 Photo-multiplier voltage (gain)

This effect is similar to that of the laser power, with different relative values because the amplification chain is not linear but logarithmic. This means that an increase in gain voltage produces noisier signals because it changes the balance between the strong signals and the weak noisy ones.

2.3.5 Burst threshold

This parameter affects burst detection, and with clean signals should be set to a low value to maximize the data rate. A higher value excludes the weaker signals, i.e., the smaller particles, biasing the average results. In a dense environment the background noise can be very strong, due to the light scattered by droplets situated on the optical path between the probe volume and the receiver: a low threshold value increases the detection of noise. If the threshold is too

low, the signal never drops below it and many bursts or even one full injection are seen as a single long incoherent event, so no droplets are detected. The burst threshold values spanned between 30 and 200 mV.

2.3.6 Signal to noise ratio (SNR) threshold

It is used to reject noisy signals, but if set to very restrictive values it results in rejection of small particles, more evident in a dense region where all signals are noisier. The available values are "High", "Medium", "Low" and "Very Low".

2.4 Signal processing and acquisition

It is useful to describe the signal processing performed by the TSI system. The scattered light signal is collected by three photomultipliers, where it is amplified by the selectable gain (0 to 1000 V). The electronic signal is then high-pass filtered (20 MHz) to remove the pedestal. In our experiment all the signals were also continuously monitored by a digital oscilloscope. Signal filtering and down-mixing can be selected to reduce the noise and the bandwidth sent to the processor section. Burst detection is performed with the variable threshold and other frequency analysis criteria, and the real-time frequency estimate obtained by the burst detector is used to select the sampling rate used for signal processing. Noisy signals can be rejected on the basis of the SNR level. Finally, a coincidence validation between the two diameter measurements can be performed, and a criterion of diameter-signal amplitude can be applied.

3. System optimization

3.1 Preliminary optical set-up

Extreme care was taken prior to any experiment in setting up the optic properly. The receiving optic was aligned onto the beam intersection with the windows in place and with the test rig pressurized, to compensate for the possible light deflection caused by the window deformation or displacement when internal pressure was applied. It was found that an incorrect alignment, in the order of a tenth of a millimeter and hence not perceivable by the naked eye, can decrease the data rate by 30% of its maximum value. The optimal alignment, normally found visually, was here defined more precisely as the position where the data rate registers a maximum when measuring a continuous steady seeded gas jet. Operatively, with the gas jet at a few meters per second and all the other operative parameters kept constant, the two iterated steps were to tune the laser power to reach a data rate in the order of 1 kHz, and then to improve the data-rate by fine aligning the receiving optic.

3.2 LDV setup in steady conditions, choice of signal filters and velocity error estimate

The steady gas jet in ambient air, without any window on the optical path, was also used to understand and optimize the band-pass filters applied prior to A/D conversion and frequency analysis, and to estimate the error committed in the velocity measurement. A set of tests was done with the steady gas jet at different velocities (the 1 and 10 m/s are reported here), and many combinations of band-pass filters and down-mix frequencies were used. The velocity range presented here is much lower than what is expected in a diesel spray, but it was chosen because it makes possible the comparison between all the filters to estimate the velocity accuracy.

Results of the velocity RMS obtained for the above-mentioned gas jet are reported in Fig. 2. As expected, the RMS is lower for narrow bandwidth filters in combination with strong down-mixing, which is applied to reduce the 40 MHz frequency added by the Bragg cell. For use with diesel spray, with velocities up to 100 m/s the larger filters must be used, and down-mixing is no longer possible. The available filters are then the 40-120 MHz (0 to 144 m/s), which has the defect of excluding negative velocities, and the 10-100 MHz (-54 to 108 m/s), which has a reduced maximum velocity but can measure negative values, and will be used in the external re-

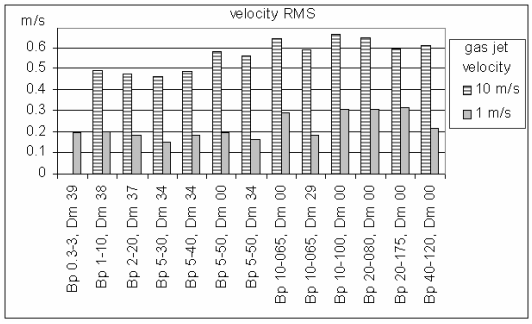

Fig. 2. RMS for two different steady gas jet velocities, and different band-pass filters and down-mix frequencies. Key: Bp 1-10 Dm38 = Band-pass 1-10 MHz, Down-mix 38 MHz.

gion of the spray, where the turbulence can generate reversed flows.

The average RMS value of the four sets at 10 m/s with narrow bandwidths is 0.48 m/s; from the high quality of these velocity results time diagram, this RMS can be considered the flow turbulence RMS_{TURB}. The average RMS value of the two large bandwidths that will be used in diesel sprays (10-100 and 40-120 MHz) is 0.65 m/s; since the measured flow is the same, the dispersion increase is attributed to the random error introduced by the larger filters, so if we accept that $RMS_{TOTAL}^2 = RMS_{FLOW}^2 + RMS_{ERROR}^2$, the dispersion introduced by the filters results in 0.44 m/s RMS, which is fairly acceptable for measurements inside the diesel spray. This is the statistical error that affects the velocity of a single particle, but cannot guarantee that no bias is present in the average. Thus the most immediate way to reduce a possible bias error is to enlarge the statistical base by increasing the measured data rate per injection.

Neither error nor bias estimate is possible for the size measure in realistic diesel conditions, since it is nearly impossible to provide a calibration flow of know droplet of that size and velocity.

3.3 PDPA setup in steady conditions, effect of windows

To test the effect of the windows, data were acquired with various configurations: without windows, with a window on the transmitting side, on the receiving side or on both, and changing the material of one window (methacrylate and borosilicate). Each time the system was re-aligned, by looking as usual for the maximum data rate, because the window thickness modifies the distance between the lens and its focusing point. For each configuration different tests were performed, to take into account the variability of results caused by the re-alignment and the possible variation of efficiency in the measurement chain. In Fig. 3 the results of data rate (droplets per second) are shown for the different window combinations. The plastic windows could maintain a higher data rate than the glass ones, so for the remaining pressurized tests the plastic windows were used.

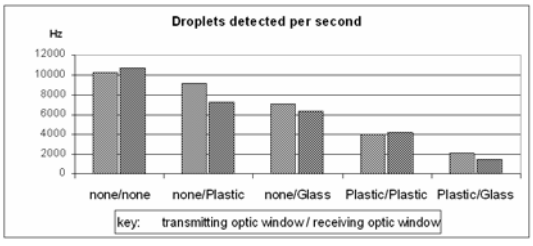

Fig. 3. Acquisition data rate for different combination of windows at the transmitting and receiving optics. Two tests are taken at each combination.

3.4 PDPA measurements in a diesel spray

The measurements performed on a diesel spray have the typical behavior shown in Fig. 4 for an injection pressure of 500 bar, which shows the droplet velocity as a function of time, measured 1.4 mm off-axis at a distance of 40 mm from the nozzle exit. Many injections are superimposed, synchronized by the trigger, to obtain sufficient data to describe them. The delay from the trigger to the first droplet is due

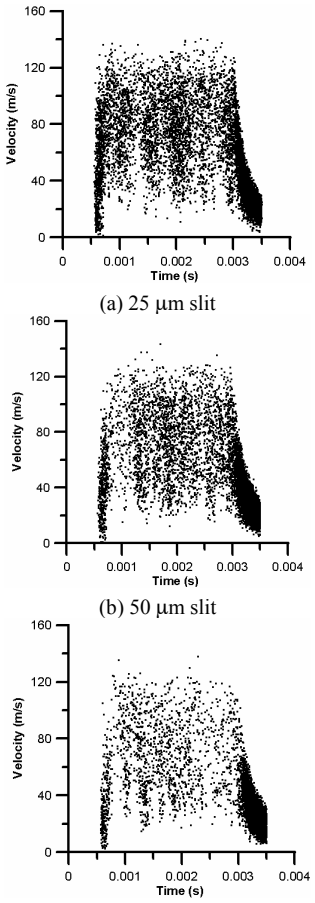

(a) 25 μm slit

(b) 50 μm slit

(c) 100 μm slit

Fig. 4. Influence of the slit aperture at the receiving optic: velocity results 40 mm downstream from the orifice, 1.4 mm off-axis, P_{inj}=500 bar, P_{amb}=7 bar (air), injection electronic pulse 2 ms.

partially to the mechanical injector delay (approx. 100 μs) and the rest to the convection time required for the droplets to reach the measurement location. The first burst of slower droplets is typical for the spray tip because they originate in the needle opening phase when the flow is restricted [11], followed by a quasi-steady period of the injection, and then by the trailing edge of the spray, caused by the injector closing. Generally, the quasi-steady period is the most difficult region to measure because of the high droplet concentration [12]. The quality of the results corresponding to this phase of the injection can be compared to the ones from the trailing edge, which is much easier to measure, and as such is the best reference for good measurements. It can be considered that the quality of the results is defined by two factors. The first is the data rate. A higher data rate means a higher proportion of the total of droplets passing through the probe volume is characterized, meaning the results should be more reliable and representative for the reality. The second is the proportion between good measurements and noise validated by the system as good measurements. If this ratio is very low, a visual inspection of the velocity measurements should reveal anomalies in the results distribution, as for example many measurements in a very narrow velocity range.

In the external region of the spray the quasi-steady phase is characterized by lower velocities, and measurements are much easier if the dense core of the spray can be avoided [8]. Consequently, if steps forward are to be made with the PDPA technique in diesel sprays, then the objective has to be to optimize the results in the difficult central region of the spray, during the quasi steady part of the injection.

3.5 Choice of the slit width

Different slits were tested to check their effect on the quality of the results. Fig. 4 shows the velocity results, obtained at 40 mm downstream from the nozzle and 1.4 mm off-axis. For each test the acquisition was stopped after 10000 droplets had been collected. If the quasi steady region is badly filled in, it means

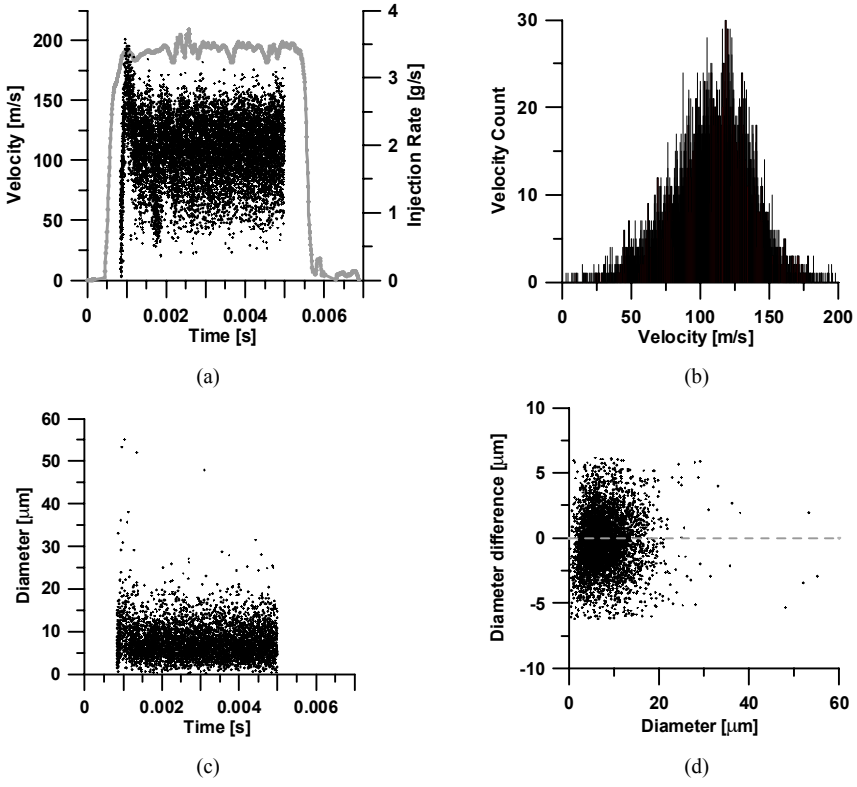

Fig. 5. Typical PDA test showing the velocity evolution in time superimposed with the instantaneous injection rate, the velocity distribution histogram, the diameter time evolution and the diameter difference vs. diameter graph. Fuel injected at 300 bar into atmospheric pressure and density, measurement point at 50 mm to the orifice, 1 mm off-axis.

that for that particular set-up it was difficult to measure, and results are mainly composed of the trailing edge droplets, which are always easy to detect. It is evident that dramatic improvement of the results when passing from the 100 μm slit to the 50 μm one, and still a marginal improvement is obtained with the 25 μm slit. In other more difficult positions with higher droplet concentration, the 50 μm slit showed further result degradation similar to the 100 μm slit, so the 25 μm slit was kept for the remaining part of the work. A test with a reduced slit height, obtained by crossing the 25 μm slit with the 50 μm one at 90º, did not show any evident improvement. It was very difficult to align, and it was preventing the evaluation of the measurement volume dimension generally performed in data post-processing, so it was not used any longer.

3.6 Control of acquisition quality

A wide set of graphic plots were always displayed during the acquisitions to check the data quality, the main ones being shown in Fig. 5. Fig. 5(a) displays the velocity evolution in time at the measuring position, as well as the injection rate on the same time base. It can be seen that the injection rate curve is longer than the acquisition time per cycle in order to measure only the quasi-steady part of the injection. The histograms of velocity (Fig. 5(b)) and frequency are used to verify that the velocity range limits are not reached; also, isolated peaks at given frequencies often indicate that noise is being detected. This noise also appears in the time encoded data as a narrow strip of velocity data (Fig. 6(a)), whose frequency is often close to a finite multiple of the Bragg cell (40, 80, 120 MHz), combined together with the down-mix frequency when applied. In Fig. 6(a) these strips occur at approximately 16 m/s and 73 m/s.

The diameter vs. time chart provides information on the size evolution during the injection (Fig. 5(c) and 6(b)), showing generally larger droplets in the initial transient phase of the injection, when the nozzle is partially closed by the needle and atomization is less efficient. However, this kind of plot alone cannot help in understanding if results are good, or, on the contrary, if noisy signals are being detected.

The diameter difference vs. diameter (Fig. 5(d)) and phase AB-phase AC scatter plots (Fig. 6(c)) give much information: if too many droplets are far from the ideal phase coincidence line (dotted line in Fig. 5(d)), this indicates poor phase estimation, the presence of non-spherical droplets, or, again, high noise levels. Droplets being biased towards one side of the coincidence line generally indicate a bad calibration of the photomultipliers, and, rarely, a problem of incorrect beam polarization. When measurements are very difficult because of high spray density, the noise becomes stronger than the smallest droplets. It can also occur that many small droplets, close to the lower size limit, are then seen as large droplets close to the maximum size limit. Such droplets are generally discarded later by applying the size-intensity validation criterion.

3.7 Effect of the laser power, burst threshold, PMT voltage, SNR

The effects of these three parameters are strictly connected, so a full set of experiments was performed in a location 0.7 mm away from the spray axis (in the direction that brings the laser path outside the spray core), at 40 mm from the tip in axial direction; fuel

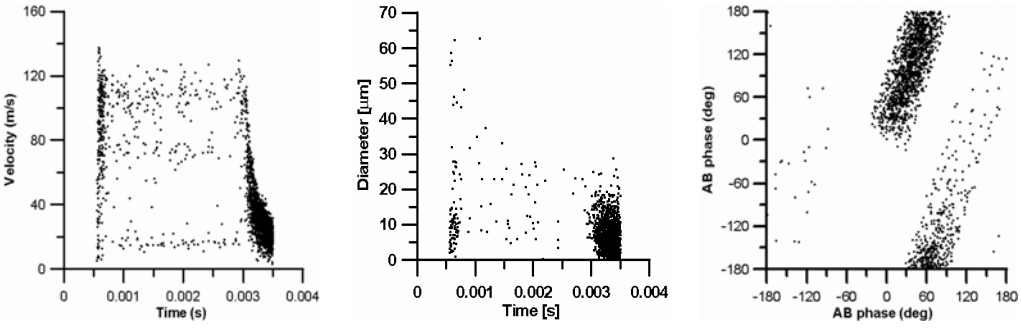

a) 25 μm slit, 50 mV burst threshold. noise in the velocity

b) 25 μm slit, 50 mV burst threshold, measured diameters

c) Phase AB- phase AC scatter plot

Fig. 6. Other plots available during acquisition and showing some of the available results.

pressure was 800 bar and gas density 14 kg/m^3. The intensity validation was enabled, eliminating as noise the droplets with a high measured diameter but very low signal intensity and vice versa, considering that normally these two factors are directly proportional. The parameter values used were:

- Laser power: 400, 600 and 800 mW (each beam power is approximately 18% of this)
- PMT voltage: 400 and 450 V
- Burst threshold: 50, 100, 150 and 200 mV
- SNR: Very Low and Medium

Only 40 of the 48 combinations were tested, since the combinations of the lowest laser power and PMT voltages resulted in very low data rate and were thus immediately excluded. In each test 10000 droplets were collected, or the acquisition was stopped after 5 minutes (2100 injections) if the data rate was too low. Many conclusions could be drawn afterwards, some of them quite obvious, others more unusual and unexpected. The results are well summarized in Fig. 7, where the data rate and the average mathematical and Sauter diameter (D_{10} and D_{32}, averaged over the whole injection time) are reported for the 40 tests.

An increase of the data rate generally means better acquisition, unless too much noise is validated as droplets, but this can be better seen in the time resolved velocity results (Figs. 4 and 6). A smaller D_{10} is generally linked to higher data rate, but again, it gives no information on the presence of noise. The Sauter diameter D_{32} follows the same trend of D_{10} unless noise is present, in this case the D_{32} can strongly increase. That is, for example, the case of BT = 50 and 100 mV, where noisy signals appear with random diameter, some of them very large so that D_{32} is strongly increased. The combination of these three parameters can be used as a good mark for setting up the system: increase of data rate and decrease of D_{10} and D_{32} are an improvement; increase of data rate and D_{32} with D_{10} decreasing means generally that noise is validated. The result of higher SNR (medium instead of very low) is generally a rejection of noise and smaller droplets, resulting in cleaner velocity profiles, but lower data rate and higher average diameter. It is also important to note that the measured average diameter D_{10} ranges here from 10 to 12 microns, meaning a 20% variation due to solely the instrument settings.

Fig. 8(a) reports the average diameters D_{10} and D_{32} of Fig. 7 expressed as a function of the data rate, for all the 40 tested conditions. While the results are quite dispersed at low data rate, the most interesting issue is that at high data rate the results are quite close together and no bias toward a preferential value is observed. This confirms again the necessity of working with the setup combinations providing higher data rate.

Fig. 8(b) reports the average velocity and RMS as a function of the data rate. All values are quite constant, with only a slightly lower average velocity and larger RMS values at low data rate. No meaningful correlation was found between average velocity and diameters.

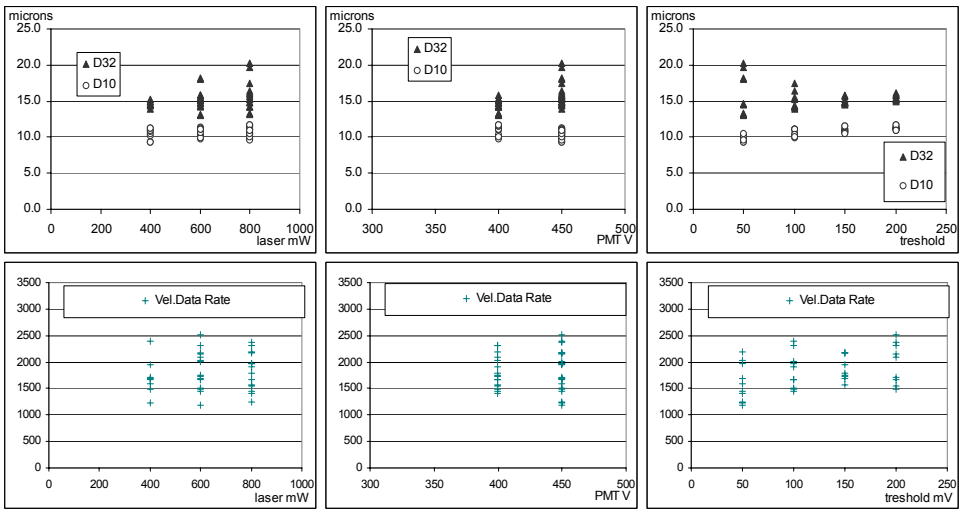

Fig. 7. Average diameter and data rate for the tested conditions. Fuel pressure 800 bar, gas density 14 kg/m^3, location at 40 mm from the spray tip, 0.7 mm off axis.

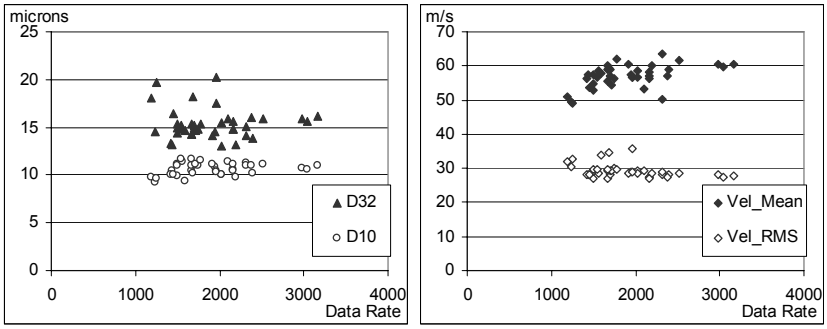

Fig. 8. Correlation between average diameter (D_{10} D_{32}), velocity average and RMS, as a function of the measured data rate, for the results of Fig. 7.

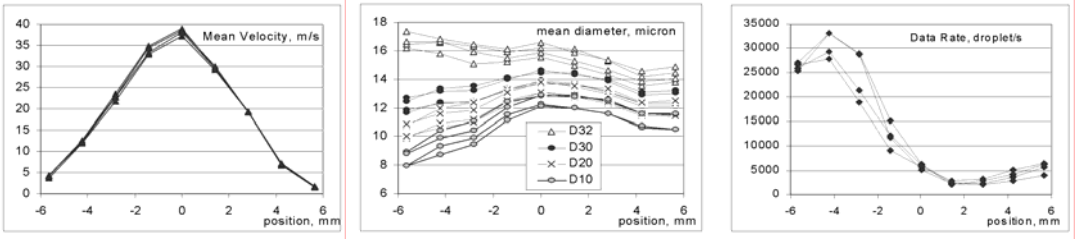

Fig. 9. Velocity, size and data rate average profiles across the spray, trailing edge excluded. Gas density 40 kg/m^3, fuel pressure 800 bar, distance from the nozzle tip 40 mm. Set up conditions: laser power 600 and 800 mW, photomultiplier voltage 450 V, burst detection threshold 100 and 150 mV.

3.8 Example of velocity and size results

As a final example of the results, the profiles of velocity, size and data rate are measured with a restricted set of four optimized set-up conditions, at different locations throughout the spray. The graphs reported in the Fig. 9 show the average profiles obtained at 40 mm from the nozzle tip, moving the measuring point across the spray, along a diameter at -45° in the scattering plane with respect to the laser beams direction, being 70° the position of the receiver. A sketch of the measuring points' location can be seen in Fig. 10. The negative axis values correspond to the side where the incident and the scattered light cross the spray with the shortest path. The averages are obtained on data from the spray tip and its quasi-steady part, by making the injection pulse longer than the acquisition window, which was 5 ms, so that the trailing edge was avoided.

The results show that the measured velocity is nearly independent of the set-up parameters. The data rate shows a weak dependence on the set-up parameters, and a strong dependence on the measurement location in the spray: inside the spray goes down to nearly 10% of the value obtained in the external parts, where the optic path is less disturbed by the dense

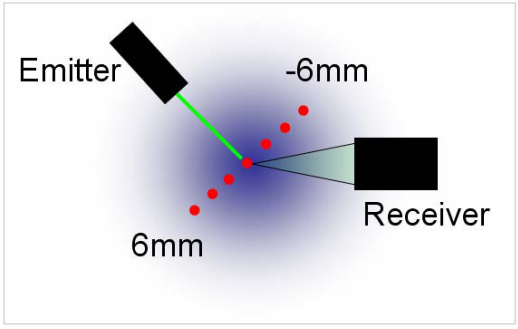

Fig. 10. Measurement points corresponding to Fig. 9.

core region. The measured diameters show the same scatter already reported in the previous paragraphs, and give an idea of the confidence that should be attributed to this kind of measurements even at 40 mm away from the nozzle exit orifice.

4. Results from a complete pdpa nozzle characterization

Although results differ when parameters are varied within a small range around what would be the ideal setup combination, given there are neither obvious noise nor measurement discrepancies, it is difficult to

pick the right combination with absolute certainty. This is the reason why it was decided to make all the tests for the nozzle characterization without changing anything in the set-up apart from the small receiver alignment required when changing the density inside the test rig. It was ensured that the set-up chosen served well throughout the entire range of test points and conditions. The chosen parameters were: PMT voltage = 450 V, Burst Threshold = 200 mV, Laser Power = 600 mW, Bandwidth Filter 40 – 120 MHz, SNR = very low, Slit Aperture = 25 μm.

The testing strategy was to measure nine points at each of the axial sections with a certain distance to the orifice, located in the same way as in Fig. 10. The measurement points were located one on-axis and the rest from the spray axis towards the receiver except for one point that was chosen on the opposite side of the spray for velocity measurement in order to check the symmetry. The measured sections were placed every 5mm from 25 to 50mm from the orifice exit. Three injection pressures were used, 300, 800 and 1300 bar, and three ambient pressures, 1.7, 4 and 6.5 bar, i.e., densities 10, 25 and 40 kg/m^3. Some combinations of geometrical position, ambient density and injection pressure could not be measured due to extreme droplet density. The nozzle characterized here has only one axisymmetric conical orifice, with 110 μm exit diameter.

4.1 Axial velocity measurements and theoretical profile

It is known by the research community that some of the equations provided by the gaseous jet theory prove to be very useful to predict some aspects of the diesel jet behavior [13]. Relying on the momentum conservation hypothesis, the velocity evolution along the spray symmetry axis can be expressed as [13, 14]:

$$u_{axis} = \frac{\dot{M}^{\frac{1}{2}}}{\rho_a^{\frac{1}{2}} \cdot \left(\frac{\pi}{2\alpha}\right)^{\frac{1}{2}} \cdot x \cdot \tan\left(\frac{\theta_u}{2}\right)}$$

Where M is the spay momentum, ρ_a is the ambient density, x is the distance to the orifice exit, θ_u is the spray's cone angle and α is a coefficient describing the shape of the radial normal distribution of the axial velocity, typically 4.6 for diesel sprays [13].

The spray momentum is measured in a special test rig [15], where due to momentum conservation the measured value is the same regardless of the distance to orifice, as long as the force sensor can collect all the spray. The spray cone angle is determined by direct spray visualization.

In the lowest density tested, as can be observed from the graph in Fig. 11, not all on-axis measurements were possible due to the spray density. The

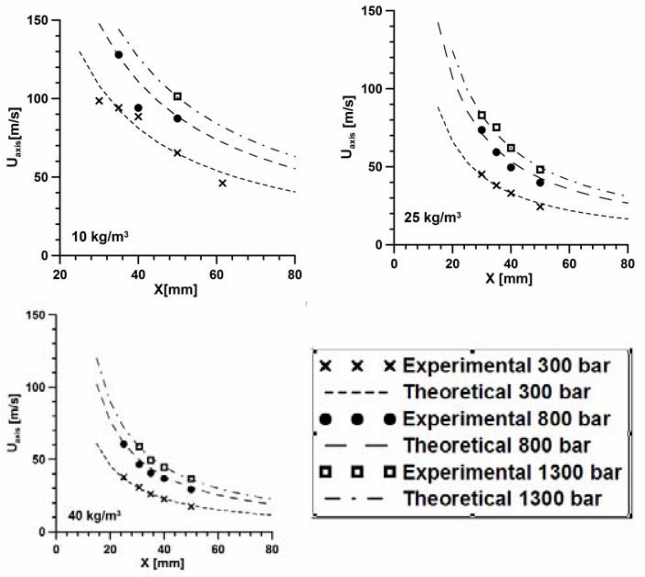

Fig. 11. Velocity on-axis measurements for different ambient density.

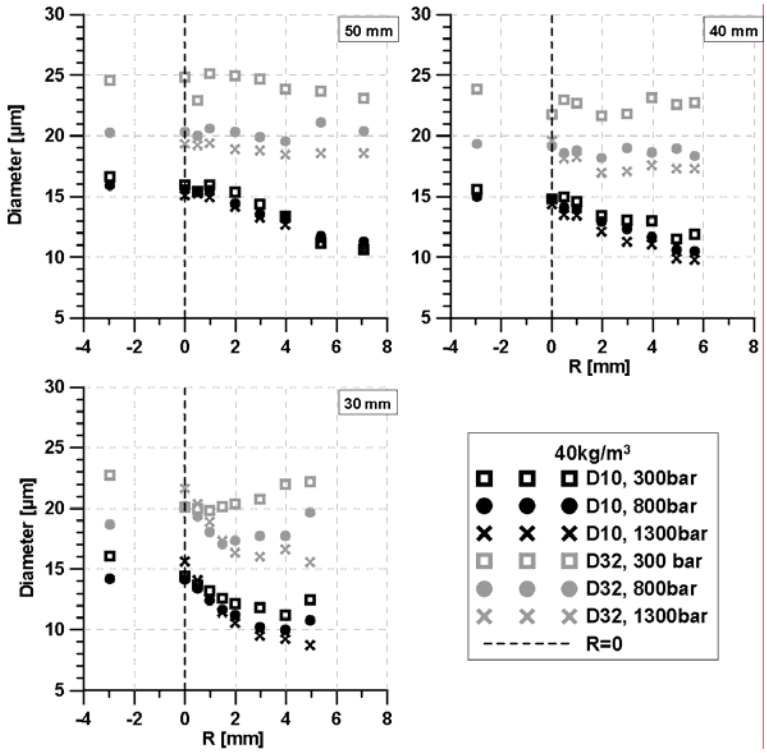

Fig. 12: Average and Sauter diameters' dependence on position and injection pressure.

closest point where measurements could be performed with 1300 bar injection pressure was at 50 mm from orifice, with 800 bar at 35 mm and with 300 bar at 30 mm. In low density conditions the spray is very narrow and the velocities are high [8]. It can also be seen that the measured values are very close to the predicted ones with the gas jet theory and information regarding the experimental spray momentum.

Also in Fig. 11 it becomes even more obvious that predicted and experimental values are very close together. For the same distances to the orifice the velocities decrease when the ambient density increases and when the injection pressure decreases, which are both natural tendencies correctly captured by the PDPA system. For the highest density it is possible to obtain measurements at 25 mm from the nozzle exit that was not possible for the low density case.

4.2 Diameter radial distribution

The average and Sauter diameters measured at various axial and radial positions with different injection pressures are presented in Fig. 12. The most obvious conclusion that can be drawn is that, in agreement with the results of other researchers [16], the increase of injection pressure reduces both the average and Sauter diameters. Another obvious tendency is for the center droplets to be on average 5µm bigger in diameter than the ones located in the spray edge. However, it seems that the spray tends to homogenize further away from the orifice, with the SMD registering practically no variation between the inner and outer part of the jet at 50 mm. It can also be noticed, especially for the SMD, that it increases slightly with the distance to orifice, most probably due to droplet coalescence.

4.3 Evaluation of the droplet density at the measurement limit

As it can be noticed from the presented results, there are some points at which the droplet density becomes too great and measurements cannot be made. It was decided to investigate further and make an estimation of the average distance between droplets at those critical points to see if the results were close and how much that distance was.

The dimensionless mass concentration on-axis is

given by: $C_{m\_axis} = \frac{U_{axis}}{U_0}$, where U_{axis} is the velocity on-axis at a certain distance from orifice and U_0 is the spray velocity at the exit. At a certain radial position r, the mass concentration is given by: $C_{m\_r} = C_{m\_axis} \cdot e^{-\alpha\left(\frac{r}{R}\right)^2}$, where R is the maximum radius of that certain spray section that directly depends on the spray angle.

It can also be shown that $C_{m/v} = \frac{\rho_f}{1 - \frac{\rho_f}{\rho_a}\left(1 - \frac{1}{C_m}\right)}$,

where $C_{m/v}$ is the mass-volumetric concentration at a certain point, expressed in kilograms of fuel per cubic meter of air-fuel mixture and ρ_f and ρ_a are the fuel and air densities, respectively.

Calculating the $C_{m/v}$ for every point where measurements were becoming extremely slow or impossible, we noticed that fuel volumetric concentration was always around 7 kg/m^3 within a ±7% variation. Judging by the measurements taken in adjacent positions we estimated that SMD was 20 μm. This means that the average droplet volume is 4.188×10^{-15} m^3. If C_v= 7 kg/m^3 then in one cubic meter of air-fuel mixture there are 8.36×10^{-3} m^3 of fuel. By dividing the two volumes it results that in one cubic meter of mixture there are 1.996×10^{12} droplets, meaning that the average distance between the droplets' centers is approximately 80 μm. To find the effective distance between two adjacent droplets, one droplet diameter must be subtracted, leading to the final result for the inter-droplet distance of approximately 60 μm. Given that the measurement volume dimension is quite similar (nominal diameter 65 μm, projected slit 30 μm), it can be deduced that in the case where the optical access to the measurement point is done through regions of lower droplet density, the multiple droplet presence inside the measurement volume is the factor that most probably determines whether measurements are possible or not. So this criterion and of the gas-jet model can be used to predict whether and where measurement will be possible in a dense spray, and to chose the most appropriate optical set-up.

5. Conclusions

A PDPA system from TSI was set up to measure the droplet size and velocity in a diesel spray. A parametric study of many setup parameters showed their influence on the acquisition results.

A very narrow slit aperture, in our case the smallest available that was 25μm, is necessary to see inside the dense part of the spray. Laser power in the range of 400-800 mW, photomultiplier amplification voltage in the range of 400-500 V and burst detection threshold of 100-200 mV were combined in order to find their optimum values leading to an increased data rate. This is almost always an indication of better results, with the limitation that beyond a certain level noise will also be detected and validated.

Several criteria that can indicate unreliable measurements were identified. Velocity results are only slightly affected by setup and can be considered very reliable, while diameter results always showed a dependence on the setup, with variation in the order of ± 10% in optimal conditions. The decreasing data rate inside the spray suggests that only a small percentage of droplets were detected and measured.

The complete nozzle characterization showed that the system works in a predictable manner and returns logical results. The velocity results proved to be correct when compared to the formulas derived from the flux momentum conservation. The diameter measurements are consistent and their tendencies in agreement with the observations of other researchers. The inter-droplet estimated distance proved on one side that the measured droplet size is very close to reality and on the other that when all parameters are chosen correctly and the slit is small enough the only factor that prevents the system from measuring in denser parts of the spray is the measurement volume diameter. The gas-jet theory can hence be helpful in the preliminary choice of the appropriate optical set-up to perform measurements in a diesel spray.

Acknowledgments

The authors would like to thank José Enrique del Rey * for his collaboration in the experimental measurements.

(*) From CMT-Motores Térmicos. Universidad Politécnica de Valencia.

This research was funded by CAVIDIESEL project; reference TRA2007-68006-CO2-01/AUT from Spanish Minister of Education and Science

Nomenclature

AB, AC : Phase differences between signals received by the light sensors A, B and C.

A/D : Analogue to Digital (conversion)
AMD : Average Mean Diameter
C_m : Mass concentration representing the ratio of the fuel mass to the total air-fuel mixture
$C_{m/v}$: Fuel mass-volumetric concentration, representing kg of fuel per m^3 of mixture
DFT : Discrete Fourier Transform
FFT : Fast Fourier Transform
LDV/LDA : Laser Doppler Velocimetry/ Anemometry
M : Spray momentum
PDPA : Phase Doppler Particle Analyzer
PMT : Photo-multiplier
RMS : Root Mean Square
SMD : Sauter Mean Diameter
SNR : Signal-to-Noise Ratio
x, y and z : Orthogonal coordinates of the measurement point, with x axis in the direction of spray penetration, and y and z axes horizontal and, respectively, vertical
u_{axis} : Droplet velocity on the spray's axis, measured in the x direction
α : Shape coefficient for the spray normal distribution
ρ_a and ρ_f : Ambient and fuel density, respectively
θ_u : Spray cone angle

Reference

[1] D. J. Timoney, J. M. Desantes, L. Hernández and C. M. Lyons, 2005, The development of a semi-empirical model for rapid NO_X concentration evaluation using measured in-cylinder pressure in diesel engines, *Proceedings of the Institution of Mechanical Engineers, P.I. Mech. Eng. D – J. Aut. Eng*. 219 (5) 621-631.

[2] G. J. Smallwood and Ö. L. Gülder, Views on the Structure of Transient Diesel Sprays, *Atomisation and Sprays*, 10 (2000) 355-386.

[3] R. Payri, J. M. Garcia, F. J. Salvador and J. Gimeno, Using spray momentum flux measurements to understand the influence of diesel nozzle geometry on spray characteristics, *Fuel*, 84 (2005).

[4] A. Doudou, and A. Maslouhi, Macro-microscopic investigation of high-pressure sprays injected by a common rail system. Journal of Mechanical Science and Technology, 21 (2007) Issue 8 1284-1292.

[5] J. Benajes, R. Payri, S. Molina and V. Soare, Investigation of the influence of injection rate shaping on the spray characteristics in a diesel common rail system equipped with a piston amplifier, *Journal of Fluids Engineering*, 127 (6) (2005) 1102-1110.

[6] J. M. Desantes, R. Payri, F. J. Salvador and V. Soare, Study of the Influence of Geometrical and Injection Parameters on Diesel Sprays Characteristics in isothermal conditions, SAE paper 2005-01-0913 (2005).

[7] H.-E. Albrecht, N. Damaschke, M. Borys and C. Tropea, Laser Doppler and Phase Doppler Measurement Techniques, 2003, XIV, ISBN: 3-540-67838-7 (2003).

[8] L. Araneo and C. Tropea, Improving Phase Doppler Measurements in a Diesel Spray, SAE paper 2000-01-2047 (2000).

[9] G. Wigley, Measurement techniques and data analyses for direct injection fuel sprays, in Phase Doppler measurements in Ultra-dense sprays, University of Darmstadt, February 2005.

[10] J. Y. Koo and J. H. Kim, 2003, Assessment of a phase Doppler anemometry technique in dense droplet laden jet, *KSME International Journal*, 17 (7) 1083-1094.

[11] C. Arcoumanis, J. Paa'l and J. H. Whitelaw, Application of Laser Techniques To Diesel Engine Sprays, 5th International Symposium on Application of Laser Techniques to fluids Mechanics, Lisbon 1990.

[12] J. Labs and T. Parker, Diesel fuel spray droplet sizes and volume fractions from the region 25 mm and below the orifice, *Atomization and Sprays*, 13 (2003) 425-442.

[13] J. M. Desantes, R. Payri, F. J. Salvador and A. Gil, Development and Validation of a Theoretical Model for Diesel Spray Penetration, *Fuel,* 85 (2006) 910-917.

[14] R. Payri, S. Ruiz, F. J. Salvador and J. Gimeno, On de dependence of spray momentum flux in spray penetration. Momentum flux packets penetration model. *Journal of Mechanical Science and Technology*, 21 (2007) Issue 7, 1100-1111.

[15] J. M. Desantes, R. Payri, F. J. Salvador and J. Gimeno, Measurements of Spray Momentum for the Study of Cavitation in Diesel Injector Nozzles, SAE Paper 2003-01-0703 (2003).

[16] Hung C. Calvin, J. K. Martin and J.-Y. Koo, Injection Pressure Effects Upon Droplet Behaviour in Transient Diesel Sprays, SAE Paper 970053 (1997).